Off-lattice Monte Carlo simulations of irreversible and reversible aggregation processes

S. Díez Orrite,*[a] S. Stoll*[a] and P. Schurtenberger[b]

Received 22nd July 2005, Accepted 23rd August 2005
First published as an Advance Article on the web 19th September 2005
DOI: 10.1039/b510449a

Monte Carlo simulations are used to get an insight into the formation of fractal aggregates from diluted to concentrated colloidal particle dispersions. Using irreversible conditions, we investigate the aggregation size distribution, architecture of the resulting fractal aggregates, possible transitions from simple aggregation to percolation and from percolation to the homogeneous aggregation regime, and discuss the fractal dimension determination from the radial distribution function. In particular the effects of the particle concentration on the aggregate fractal dimensions are considered. Reversibility is also introduced in the model so as to consider more realistic systems. The effects of aggregate fragmentation and internal reorganization are then investigated by adjusting the interparticle interaction potential. Important results dealing with the concomitant effect of aggregate break-up and internal reorganization on the aggregate local structure and stability with regards to phase separation are discussed.

Introduction

Dispersed colloidal particles (as solid inorganic and organic particles) under the influence of attractive forces such as van der Waals or depletion interactions, for example, build characteristic structures whose size increases with time. Due to the importance of this phenomenon in industrial systems (for example in the development of homogeneous dispersions) and environmental processes such as waste water treatment, many theoretical and experimental studies have focused on the understanding of the destabilization of colloidal dispersions.

Aggregates, which are usually defined as assemblages formed from the aggregation of elementary spherical particles, exhibit geometrical properties that can be conveniently described using the fractal geometry.[1] In general, fractals can be defined as disordered self-similar systems with a non-integer dimension. It should be noted that scattering experimental methods are widely used to characterize such structures, in particular for determination of the fractal dimension, which gives a quantitative description of the packing of the particles within the aggregates and is expected to explain the rheological and mechanical aggregate properties. These methods have shown that the value of the fractal dimension, D_f, may vary depending on the experimental conditions; $D_f = 1.75$ when the aggregation process is controlled only by the diffusion of the particles or formed aggregates,[2] while $D_f = 2.02$–2.12 when a large number of collisions are required before particles and aggregates form irreversible bonds.[3]

During the past two decades important progress in the understanding of the aggregate structures and kinetics have been made using more or less sophisticated computational models based on Monte Carlo or Brownian dynamics.[4–13] Among them, the diffusion limited cluster–cluster aggregation model (DLCA) is the most widely used model for the understanding and calibration of aggregation and aggregate growth of colloidal suspensions. The ramified fractal aggregates obtained from the DLCA model exhibit a value of the fractal dimension close to 1.75, which is in good agreement with the ramified colloidal aggregate structures formed in fast aggregation processes. Nonetheless, more compact aggregates can be obtained by decreasing the value of the sticking probability (p) to form a bond between particles. Thus, when p is approaching zero, because of the presence of electrorepulsive interactions between the particles for example, the value of the fractal dimension is increased to 2.08, which describes well the experimental aggregates formed through slow aggregation processes. This modified DLCA model is known as the reaction limited cluster–cluster aggregation model (RLCA). Both DLCA and RLCA aggregation models represent two universal aggregation processes.

However, there is experimental evidence,[14] at least on short length scale, that other phenomena are expected to play a role. Under certain experimental conditions, such as aggregation in a secondary minimum, initial aggregates obtained by DLCA mechanism can restructure to more compact structures after a certain time. This behaviour has been observed in diluted colloidal systems with small silica or gold particles where the value of the fractal dimension increases from 1.75 to 2.1[15] and 2.4,[16] respectively. Although these aggregates seem to be equivalent to those obtained at low values of the sticking probability, the RLCA model cannot account for the restructuring of the aggregates due to the irreversible nature of the interparticle bonds and absence of restructuring.

In order to account for such processes, several models have been proposed modifying the classical aggregation models. Hence, restructuring processes through rotations of the rigid

[a]*Department of Inorganic, Analytical and Applied Chemistry, Analytical and Biophysical Environmental Chemistry (CABE), University of Geneva, Sciences II, Quai Ernest-Ansermet 30, CH-1211 Geneva, Switzerland. E-mail: silvia.diez@cabe.unige.ch; serge.stoll@cabe.unige.ch*
[b]*Department of Physics, University of Fribourg, Chemin du Musée 3, CH-1700 Fribourg, Switzerland. E-mail: peter.schurtenberger@unifr.ch*

clusters about their contacting particles were proposed to increase the number of contacts between aggregates.[17–19] However, the probability of aggregate reorganization was found to be limited due to the irreversible nature of the clusters formed. Furthermore, the fractal dimension was not dramatically changed (between 2.09[18] and 2.19[19]) since the restructuring mechanism was limited to short distances.

P. Meakin[20] and M. Kolb[21] proposed a reversible aggregation model where they modified the original DLCA model by including random bond breaking. Thus, while the results obtained from Meakin's model indicated a weak effect on the fractal dimension, in the case of Kolb the random bond breaking model resulted in an increase of D_f to 2.03, in agreement with the restructuring found in silica aggregates.[15] The evolution of D_f with simulation time was not observed.

To achieve a more realistic reversible aggregation model which involves the rearrangement of particles from energetic consideration rather than geometric rules, off-lattice[22] and lattice growth models[23–26] have been proposed by modifying the DLCA model, including finite interparticle attraction energies. These studies demonstrated that the reversibility condition plays an important role both in the aggregation kinetics and aggregate structures. Depending on the interparticle bonding energy and simulation time considered, aggregates can be ramified, with a fractal dimension corresponding to the DLCA model or exhibit much more compact structures in agreement with some experimental results.[27–29]

In this paper we present a detailed and systematic analysis of the influence of parameters such as the particle concentration by focusing on the behavior of concentrated systems and interparticle attraction energy which are expected to profoundly influence the structural properties and evolution rate of the aggregate formation. We will also try to answer a number of open and fundamental questions dealing with: (i) the change or not with the particle concentration of the aggregate fractal dimension formed in DLCA conditions, (ii) the presence (or not) of successive aggregation regimes during time depending on the particle concentration, and (iii) how reversibility and the introduction of finite bond energies are supposed to influence aggregation rates and aggregate structure. To answer these questions, fractal dimensions, radial distribution functions and average aggregate numbers are calculated and discussed. This study is carried out using an off-lattice cluster–cluster algorithm, under both diffusion-limited (DLCA) and reversible (modified DLCA model with finite bonding energy) conditions using the Monte Carlo simulation method.

The outline of this paper is as follows: In Section I we will introduce both irreversible and reversible aggregation models used in this work; Section II deals with the numerical results obtained under irreversible and reversible conditions; conclusions are reported in the Section III.

Models

A. Irreversible aggregation

Initially, i non-overlapping identical spherical colloidal particles are positioned randomly in a cubic box of edge length L according to the chosen volume fraction ϕ, $\phi = (i/L^3)v_p$, where v_p represents the volume of a colloidal particle. Periodic boundary conditions are used. Then particles and aggregates (also referred to as clusters), formed during the aggregation process, diffuse according to Brownian motion (random walk). Particle and cluster displacements are chosen in such a way that the allowed maximum step size is equal to the radius of a colloidal particle.[30] We assume that particles and clusters have the same mobility since this condition does not change significantly the scaling properties[5,23] and is expected to considerably reduce the MC simulation time. The particle interaction is described by a square-well potential including hard-sphere repulsion where the well depth goes to infinity while the well width is given[22] by the parameter D whose value is equal to $D = 1.1d$; d represents the diameter of the colloidal particle. The use of this square-well potential allows a clear and unambiguous definition of the number of colloidal particles that form part of the aggregates and is expected to be well adapted for modelling depletion aggregation processes, for example, where the square-well depth is proportional to the polymer concentration and the width proportional to the polymer molecular weight.

Once two particles are connected, the bond is not broken during the aggregation process so as to mimic irreversible conditions. No further restructuration or aggregate reorganization is considered. During the simulation, one or more clusters can appear, depending on the particle volume fraction, spanning the simulation box and hence promoting gelation. In our simulations gel formation is considered as achieved when the largest aggregate spans the box from edge to edge in the three space directions. When all particles of the system are connected to a single cluster, the simulation is stopped.

B. Reversible aggregation

To mimic reversible aggregation conditions every Monte Carlo step is divided into two parts. The first part corresponds to the diffusion and formation of DLCA clusters, whose details have been explained above. Once all the particles and clusters of the system have been moved, the second part of the Monte Carlo step is switched on, in which we simulate the thermal motion of the particles within aggregates.

The inter-particle interaction is now given by this square-well potential:

$$U(r)\begin{cases}\infty & r<d\\ -\varepsilon & d\le r\le D\\ 0 & r>D\end{cases} \quad (1)$$

where d represents the diameter of colloidal particle, D the attraction range given by the relation $D/d = 1.1$ and ε the square-well depth, whose value is adjusted between 0.5 and 10 kT.

Particle movement gives a change in energy $\Delta E(r)$ whose probability is proportional to $\exp(-\Delta E(r)/kT)$, where k represents the Boltzmann constant and T the temperature of the system. Any attempted move consistent with the non-overlapping restriction is accepted considering the Metropolis rule:[30] $\gamma < \exp(-\Delta E(r)/kT)$, where γ is a random number uniformly distributed between zero and unity. According to this condition, the aggregation and reversible process evolves

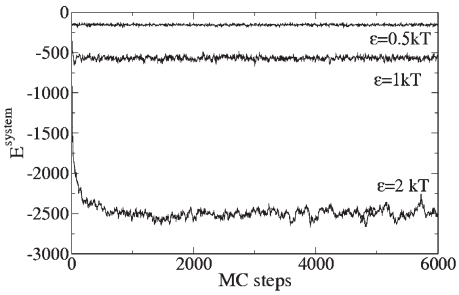

Fig. 1 Variation of the total energy with time (considered as MC steps) for ε values equal to 0.5, 1 and 2 kT at $\phi = 0.1$. In the three cases, according to the Metropolis condition, the system approaches an equilibrated state after $\sim 2 \times 10^3$ MC steps.

until a thermal equilibrium state is reached (see Fig. 1.). Like in irreversible aggregation process, the evolution time is measured in MC steps where one MC step corresponds to the movement of all particles and clusters within the simulation box.

Results

A. Irreversible cluster–cluster aggregation process: DLCA process

The ramified aggregates obtained from the DLCA model are characterized with a fractal dimension close to 1.75 in very diluted conditions, *i.e.*, when the distance between clusters is bigger than their size (flocculation regime). However, when particle concentration increases the situation changes in particular upon approaching the gel point. At large length scales, it is not clear if clusters begin to aggregate homogeneously (showing a value of D_f equal to the space dimension) and/or if they only "percolate", with a value of D_f close to 2.5 which corresponds to an "infinite" percolating cluster in 3D.[10,31]

In order to clarify this point and considering that the fractal dimension D_f of aggregates can be obtained from the scaling relation[32]

$$N \propto R_g^{Df} \quad (2)$$

we have calculated for different particle concentrations the aggregation mass N as a function of the mean square radius of gyration of the clusters $<R_g^2>$ obtained during several aggregation processes.

In very diluted conditions (Fig. 2.), the best fit of the data gives a fractal dimension equal to 1.77 ± 0.02, which is in good agreement with the DLCA aggregation process. However, the plot obtained at larger particle concentrations can obviously not be described by only one scaling parameter. In Fig. 3, the data obtained at four different particle concentrations are presented. The solid and dashed lines have slopes corresponding to the expected power law behavior of clusters formed in diluted conditions and percolating clusters respectively. As observed, there exists a transition between two regimes that happens at smaller values of N when the particle concentration increases. This transition can be characterized by N_c and R_{gc}^2, where the limiting slopes cross. If we normalize N and R_g^2 by

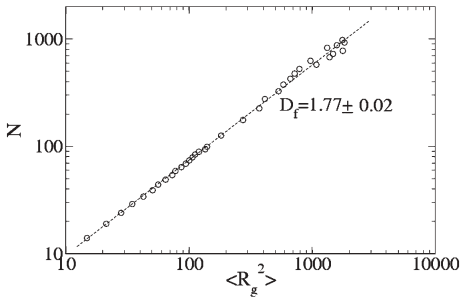

Fig. 2 Aggregate mass, N, *versus* mean square radius of gyration $<R_g^2>$ (excluding values of $N < 5$) for a volume fraction $\phi = 5.24\ 10^{-4}$. The data result from an average over 100 simulations.

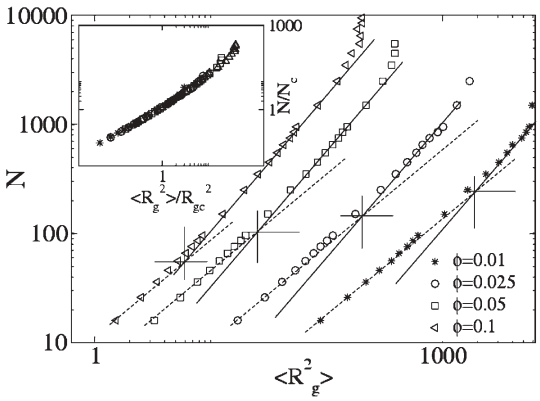

Fig. 3 Relation between the aggregate mass and the mean square radius of gyration of clusters obtained during a DLCA process at different concentrations: $\phi = 0.01$ (*), $\phi = 0.025$ (○), $\phi = 0.05$ (□) and $\phi = 0.1$ (◁). The solid lines indicate the expected power law behavior for percolating clusters, while the dashed line indicates the expected behavior in diluted conditions. Inset: Master curve obtained from the data presented above by normalizing N and R_g^2 with the characteristic aggregation mass (N_c) and radius (R_{gc}^2), found for each concentration. The data result from an average over 100 simulations.

the corresponding N_c and R_{gc}^2, the results at different concentrations superimpose as shown in the inset. This superposition indicates to us that this transition between the two regimes does not depend on the particle concentration considered or aggregate sizes but only on the level of interpenetration between the aggregates.[10] Furthermore, the observed gradual change of the slope suggests to us that a single fractal dimension does not characterize, over all length scales, the structure of large clusters formed close to the gel point. Thus, on length scales less than R_{gc} aggregates show a value of D_f corresponding to the DLCA process (diluted conditions), while on length scales bigger than R_{gc}, the value of D_f increases as expected for percolating clusters.[10]

Experimental studies of colloidal gels have shown the presence of different regimes in the description of colloidal gel structure formation.[33] Therefore, at large length scales, an additional regime where the gel becomes homogeneous should be considered. In Fig. 4 the values of N and $<R_g^2>$ corresponding to $\phi = 0.05$ and 0.1 (where the expected change of the slope is perceptible) are plotted. The solid and dashed lines have slopes corresponding to the expected power law

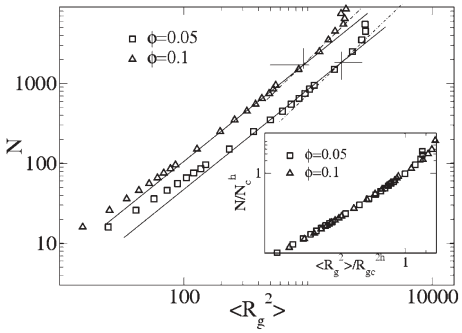

Fig. 4 Aggregate mass and mean square radius of gyration of clusters obtained at $\phi = 0.05$ (□) and 0.1 (△). The solid and dashed lines indicate the expected power law behavior for percolating clusters and homogeneous aggregation, respectively. Inset: Master curve obtained from the data presented above by normalizing N and $<R_g^2>$.

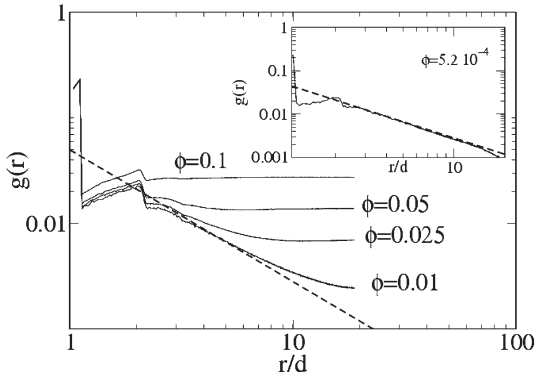

Fig. 5 Radial distribution functions obtained from final aggregate at different concentrations. Curves result from an average over 100 simulations. The inset shows the $g(r)$ function corresponding to one aggregate at $\phi = 5.24 \times 10^{-4}$. In both figures, the dashed line has a slope equal to −1.25.

behavior of percolating clusters ($D_f = 2.5$) and homogeneous clusters ($D_f = 3$) respectively. Each curve can be characterized by N_c^h and R_{gc}^{2h} where both lines cross. As shown here the transition between the percolating and homogeneous regimes happens at smaller values of N when the particle concentration increases. If the data are normalized by their corresponding N_c^h and R_{gc}^{2h} values, again both plots superimpose, as shown in the inset of the figure.

In the literature, several authors have tried to derive D_f from the aggregate structures using the radial distribution function $g(r)$.[9,34,35] One important point in these studies was to determine if the aggregate fractal dimension changes with the particle concentration for a given aggregation mechanism. Unfortunately, we demonstrate here that the $g(r)$ function can not describe correctly the structure of the aggregate at large particle concentrations and consequently the derivation of D_f from $g(r)$ is often erroneous.

We computed the radial distribution function, in order to investigate the structure of the simulation system as a whole, *i.e.*, not just the fractal structure of individual clusters. The $g(r)$ function is defined as $g(r)\rho dV$ = the number of particles in the volume element dV at distance r from a given particle center, ρ being the system number density. This function is normalized with the number density of the system. So, for a system that is homogeneous beyond some length scale r, the $g(r)$ function reaches the value of 1.0.

The $g(r)$ function can be divided in three regions: The first region ($1 \leqslant r/d \leqslant 3$), known as the non-fractal region of the cluster,[9] is formed by a large peak ($r/d = 1$), whose value is related to the average number of particles that are directly bound to a given particle, and by a discontinuity ($r/d = 2$) caused by the contribution of the next nearest connected neighbors, whose importance decreases when the particle concentration increases. At larger distances ($r/d > 3$), the fractal region is approached, where the function decreases with a power law $r^{(3-D_f)}$. After this power law regime, $g(r)$ exhibits a minimum, whose position indicates the correlation length of the aggregate, ξ, which is representative of the characteristic size of the aggregate. Upon further increasing r ($r/d > \xi$), $g(r)$ approaches the homogeneity regime, *i.e.*, approaches a value of 1.

Fig. 5 shows the pair correlation functions obtained at the end of the simulation runs for different volume fractions. In very diluted conditions, $\phi \sim 10^{-4}$, the fractal part of $g(r)$ decreases as a power law with an exponent equal to −1.25, giving $D_f = 1.75$, in good agreement with what we expect in diluted DLCA conditions. However, the analysis of the $g(r)$ at higher particle concentrations shows a different behavior. In such conditions, the r range over which the fractal exponent can be determined with some accuracy dramatically decreases when the particle concentration increases. The $g(r)$ function exhibits a large deviation with respect to the dashed line (slope −1.25, obtained using $D_f = 1.75$), while it becomes much more visible when particle concentration increases. In such conditions, the fit of $g(r)$ to a power law gives lower exponents over some range of r, hence larger apparent values for D_f are derived.

Lattuada *et al.*[9] derived D_f by fitting $g(r)$ to a power law in a very small range $3 < r/d < 4$ and concluded that the compactness of colloidal gels increases with the particle concentration. Our results suggest that for $\phi > 2\%$, due to the mathematical continuity of the $g(r)$ function imposed by the homogeneity regime, it is very difficult to distinguish a power law dependence as well as to extract a correct value of the fractal dimension in the fractal domain. In consequence, it is difficult to attribute higher fractal dimensions to aggregates formed at large concentrations.[35] Furthermore, we also believe that there is no reason for an increase or decrease of D_f as the DLCA aggregation rules are not modified with the increase of the particle volume fraction.

B. Reversible cluster–cluster aggregation process

The main difference between DLCA and reversible aggregation processes comes from (i) the possibility to break up the connections between colloidal particles and aggregates (fragmentation mechanism) and (ii) the reorganization within the aggregates during the aggregation process (restructuring mechanism). Thus, while in DLCA the simulation is stopped when all particles of the system are connected to a single cluster, in reversible aggregation conditions the connections

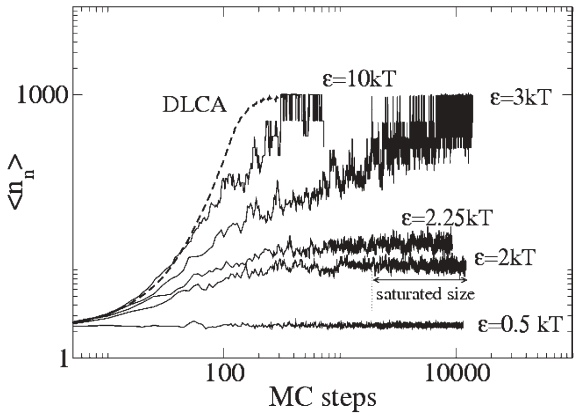

Fig. 6 Variation of the number average mean aggregate size ($<n_n>$) with the simulation time (MC steps) at $\phi = 0.05$. In reversible conditions, a plateau is observed at large MC steps, which suggests the presence of both aggregation and fragmentation mechanisms in the process.

between particles (or aggregates) can break up, produce small fragments and change the particle positions repeatedly, reaching an equilibrium distribution of aggregate structures at larger MC steps.

To illustrate this, the evolution of the mean aggregate size during reversible aggregation processes is plotted in Fig. 6. The number average mean aggregate size is defined as $<n_n> = M_1/M_0$, where $M_i = \Sigma_n^i N_n$ is the ith-order moment of the size distribution.[28] Aggregation is obviously favored by increasing the inter-particle energy. However, after an equilibrated period, a plateau is observed at large MC steps in almost all the situations. This plateau suggests the presence of a concomitant fragmentation–aggregation process, whose relative importance depends on the ε value considered. For small ε values ($\varepsilon \sim 0.5$ kT) the influence of the fragmentation mechanism is so high that clusters do not have time to grow before they break.[24] For larger ε values, despite the fact that the aggregation mechanism is promoted, the equilibrium state[26] seems more difficult to achieve. Indeed, in comparison with the variation of $<n_n>$ obtained from the DLCA model, the average mean aggregate size obtained at high attractive interparticle energies initially resembles that obtained by irreversible conditions, because aggregation occurs much faster than fragmentation and/or restructuring. Nonetheless, significant changes in the aggregate structures are observed at long simulation time mainly due to the slow effect of aggregate restructuration.

The relative importance of restructuring can be investigated through the average number of particles connected to a given particle, $<z>$. In DLCA simulations, because of the irreversibility condition, no loops can be formed during the aggregation process and only binary collisions between particles are allowed, independently of the colloidal particle considered.[10,19] However, the situation is different under reversible conditions. Fig. 7A presents the $<z>$ variation obtained at different ε values when $\phi = 0.05$. For small ε values the influence of the fragmentation mechanism is quite important. As demonstrated in Fig. 6, aggregates have no time to grow before breaking, and hence the number of neighbors around a given particle is quite

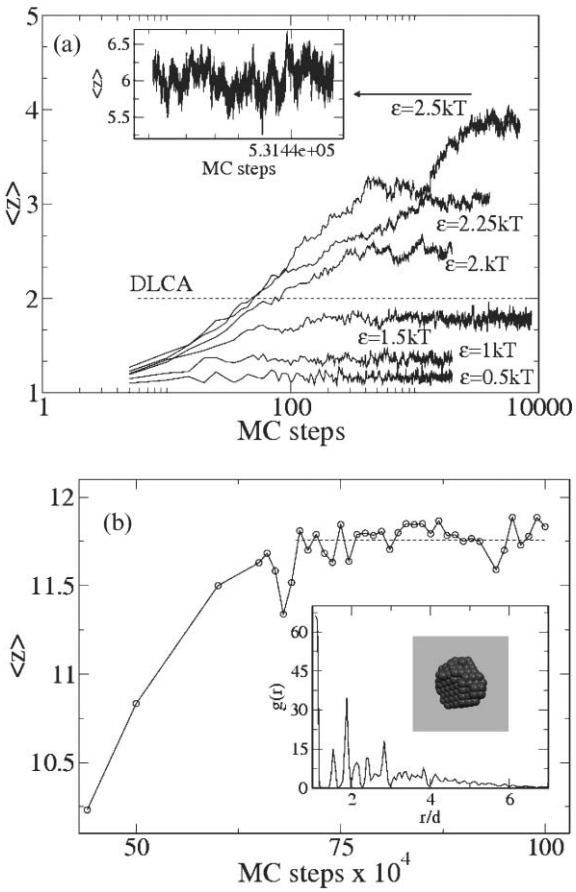

Fig. 7 (A) Variation of mean number of neighbors $<z>$ with the MC simulation time, considering different values of ε at $\phi = 0.05$. The $<z>$ value is strongly related to the finite bond energy. At small values of ε, fragmentation mechanism makes aggregates to break so quickly that the values of $<z>$ are quite small. At large values of ε, although aggregation is promoted, restructuring and fragmentation mechanisms increases the aggregate compacticity, obtaining higher values of $<z>$. (B) Time evolution of $<z>$ and plot of the $g(r)$ function obtained at $\phi = 0.05$ and $\varepsilon = 3$ kT. After a given MC step, $<z>$ plot saturates at values around 11.8, being representative of the maximum number of neighbors allowed by geometrical packing.

small and can be even less than 2 which corresponds to the DLCA process value.

By increasing ε, at large simulation time, more compact aggregates are clearly formed. When $\varepsilon \geqslant 2kT$, $<z>$ exhibits higher values at equilibrium than $<z^{DLCA}> = 2$. Despite the fact that aggregation is promoted, restructuring, and to a less extent fragmentation, is expected to increase the aggregate compactness.

These mechanisms ultimately influence not only the stability of the colloidal dispersion, but also can induce phase separation, promoting the emergence of a multiphase type system. Depending on the concentration and interparticle interaction, the system can exhibit a liquid–gas coexistence and separate into one phase with high density (liquid or solid) and another with a low density (gas). Investigating partially the phase diagram, we calculated that, for $\phi = 0.05$, the aggregation process with $\varepsilon = 2.25kT$ is close to a phase separation.[36] Increasing the interparticle interaction to $\varepsilon = 3kT$,

the colloidal system is driven into a two-phase separation, characterized by the formation of compact droplets (dense phase) and free colloidal particles (gas phase) around it. In these conditions, the grade of compactness of the aggregate has become so important that a close-packed structure is achieved. In Fig. 7B, the time evolution of $<z>$ obtained at $\varepsilon = 3kT$ and $\phi = 0.05$ is represented. As observed, the average number of neighbors approaches values close to 12, which is representative of the maximum number of neighbors allowed by geometrical packing. Although this point will be developed in a future paper, it is interesting to indicate the characteristic shape of the pair correlation function obtained in such conditions. As shown in the inset, sharp peaks forms part of the $g(r)$ plot indicating a short-range crystalline-type ordering within the aggregate, in agreement with results found in the literature in such conditions.[22]

To illustrate the influence of reversible aggregation on aggregate structures and final colloidal system state, Fig. 8 shows snapshots obtained for the same simulation time at four different ε values. A ramified DLCA aggregate is considered as the starting configuration. When $\varepsilon = 0.5kT$, the initial DLCA aggregate is broken into very small aggregates (frequently dimers) as well as free colloidal particles (Fig. 8A). On the other hand, the increase of the interparticle energy at $\varepsilon = 2.5kT$ promotes the aggregation between colloidal particles. Larger aggregates are formed, however the fragmentation process still influences the colloidal system (there are a quite number of free particles in the fluid phase as shown in Fig. 8B). The combination of both mechanisms (fragmentation and aggregation) results in aggregates which are quite compact (see the largest aggregate obtained at $\varepsilon = 2.5$ and $3kT$). These near-compact droplets again suggests us the formation of phase separation in the colloidal system.[24,36]

At very high values of bond energy ($\varepsilon = 5kT$), the aggregation occurs at a faster rate than fragmentation. Here the probability for bond fragmentation is less important so the resulting aggregate looks more ramified compared to those obtained with smaller bond energy at the same simulation time. However, due to the finiteness of the attractive interaction, the probability of reorganizing within the aggregate is still possible. This is illustrated by the resulting aggregate structure in Fig. 8D, which is clearly more compact at short length scales ($<z> \sim 5$) than the starting DLCA aggregate ($<z> = 2$). This also suggests a slow and continuous increase of the fractal dimension resulting in D_f value higher than 1.75.

Shih *et al*,[23] using a 2D simulation model, also demonstrated that, at high interparticle interaction energy, the fractal dimension was close to the DLCA value for a long period of time. In fact, the structure of the resulting aggregates may look frozen at large length scale (and hence exhibit a kinetic stability), but it continuously changes by particle reorganization at short length scale, hence affecting in a second step the value of the fractal dimension to reach at the end a thermodynamic stability.[15,16]

To investigate the time evolution (where the time is measured in MC steps) of D_f in reversible conditions, at a given particle concentration, in a first time DLCA aggregates were generated. Then reversibility was switched on and the fractal dimension, corresponding to different moments of the reversible aggregation process, was calculated from a log–log plot of N *versus* R_g, assuming that aggregates are still fractal during the reversible process.[29]

In Fig. 9 the cluster sizes corresponding to the interval $20 \leqslant N \leqslant 200$ for $\phi = 0.01$ and $\varepsilon = 3kT$ at three different moments of the aggregation process are plotted; each point is the result of averaging over ten samples. From this figure we observe how the aggregate structure becomes more compact

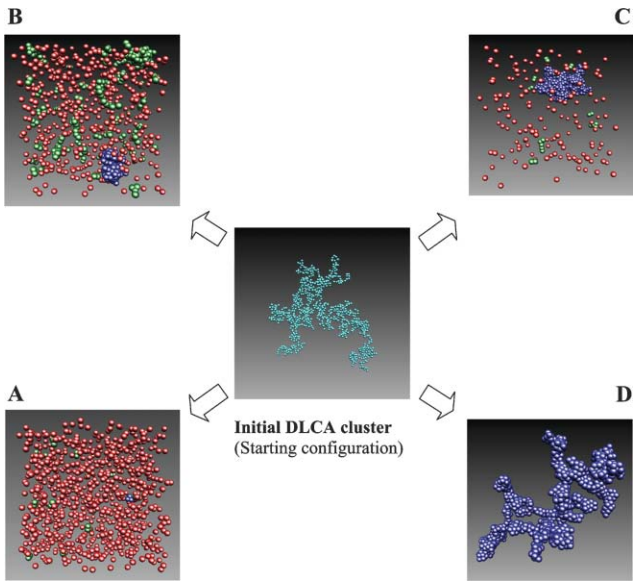

Fig. 8 Influence of the interparticle energy ε value on the aggregation process: (A) $\varepsilon = 0.5kT$, (B) $\varepsilon = 2.5kT$, (C) $\varepsilon = 3kT$ and (D) $\varepsilon = 5kT$. These snapshots were obtained at $\phi = 0.01$ and the same simulation time. A ramified DLCA aggregate is considered as the starting configuration. Red and green colors represent free colloidal particles and aggregates respectively, while blue color indicates the biggest aggregate. From these results a phase separation in the colloidal system may be observed, depending on the bond energy.

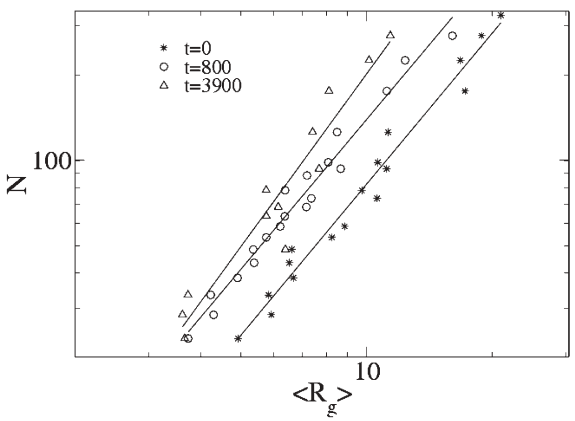

Fig. 9 Plot of N *vs* $<R_g>$ at three different moments of the aggregation process. The data corresponding to $t = 0$ is representative of the initial DLCA distribution size. From this plot, it is observed that for a given aggregate size, the $<R_g>$ value is continuously decreasing with time, indicating the continuous increase of the degree of compactness of the aggregates once reversibility is switched on. Each point is the result of averaging over ten samples. System conditions: $\phi = 0.01$ and $\varepsilon = 3kT$.

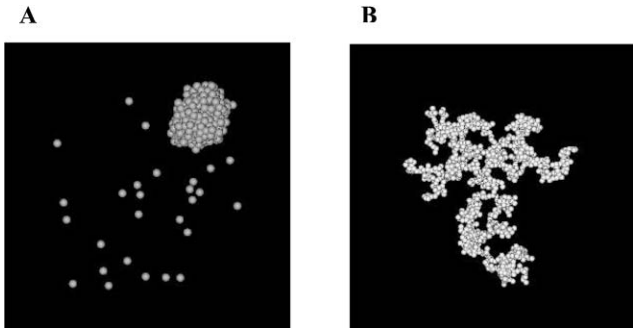

Fig. 10 (A) Snapshot of phase-separated aggregated system obtained at $\phi = 0.01$ and $\varepsilon = 3kT$. (B) Final aggregate obtained by DLCA mechanism at $\phi = 0.01$.

while aggregation including reversibility proceeds, increasing thus the value of the fractal dimension from 1.75 at the beginning of the simulation process ($t = 0$ where t is measured in Monte Carlo steps) to 2.03 at $t = 3900$. As shown in Fig. 10, once the colloidal system, including reversibility, reaches the equilibrium ($t \gg 3900$) (i) final aggregates are much more compact with fractal dimensions close to 3 and (ii) the system separates in droplets and individual particles. Thus, while two scaling regimes are expected to describe the aggregate structure of irreversible DLCA systems, at this particle concentration, for a reversible system the final aggregation picture is somewhat different and much more complicated owing to continuous changes in the fractal dimension and possible phase separations.

Conclusions

Monte Carlo simulations were used to get an insight into the formation of aggregates from particle dispersions. Parameters such as particle concentration and interparticle attraction energy have been considered to study the variation of the structural properties such as the fractal dimension and aggregation regimes. Diffusion limited cluster aggregation has been considered in the first part of the paper. Different regimes were found in the description of the aggregate structure depending on the particle concentration. In very diluted conditions, the ramified aggregates can be characterized with a fractal dimension close to 1.75 whereas, in non-diluted conditions, the structure of aggregates can not be described by a single fractal dimension due to the grade of interpenetrating between clusters before connecting. The plot of N *vs* $<R_g^2>$ showed the presence of three regimes characterized, from small to large length scales, with $D_f = 1{,}75$, 2.5 and 3 corresponding to DLCA, percolating and homogeneous aggregates, respectively. Our results, obtained at different values of particle concentration, indicate that the regime transition happens at smaller values of N when the particle concentration increases. Therefore, in the calculation of D_f from the $g(r)$ function, at particle concentration $\phi > 2\%$, it is very difficult to see a power law dependence and consequently attribute a correct value of the fractal dimension in these conditions. In this way, we conclude that there is no reason for an increase or decrease of D_f with the particle concentration.

A modified DLCA model was also considered to mimic the reversible aggregation conditions. Our results have shown that the interaction between particles plays an important role in the aggregation process. Thanks to the finite attraction energy, the possibility to break up the connections between aggregates and colloidal particles (fragmentation mechanism) or the reorganization of particle positions within aggregates (restructuring) means that (i) aggregates can not grow infinitely (ii) the aggregate structure becomes more compact. Our results have demonstrated that the importance of both mechanisms and their influence not only affect the stability of these systems but also can induce the formation of phase separation. Thus, while at small values of ε, aggregates break up before growing, at big values of ε, both restructuring and aggregation promote the formation of spherical or ramified aggregates, depending on the bonding energy, with a grade of compactness bigger than DLCA aggregate structures. It is shown that computer simulations can isolate in good agreement the factors that control the destabilization of colloidal particle solutions and, thus, can help addressing the optimization of particle–polymer mixtures where aggregate depletion and reversible conditions are expected to play a key role. We are currently extending our investigations to the calculation of the full domain phase diagram and fractal dimensions determination in reversible conditions.

Acknowledgements

The authors are grateful to Manuel Rotterdau, Jean Christophe Gimel, Giuseppe Foffi, Francois Muller, Hervé Dietsch, Mirko Saric and Beat Keller for their encouraging and stimulating discussions. S. D. O. also wants to acknowledge Dr E. Leontidis for her visit in his research group. Financial support was provided by the Commission Suisse pour la Technologie et l'Innovation (CTI), Project no 6056.2

References

1 B. B. Mandelbrot, in *The Fractal Geometry of Nature*, ed. W. H. Freeman, New York, 1983.
2 P. Dimon, S. K. Sinha, D. A. Weitz, C. R. Safinya, G. S. Smith, W. A. Varady and H. M. Lindsay, *Phys. Rev. Lett.*, 1986, **57**, 595.
3 D. A. Weitz, J. S. Huang, M. Y. Liu and J. Sung, *Phys. Rev. Lett.*, 1985, **54**, 1416.
4 T. A. Witten and L. M. Sander, *Phys. Rev. Lett*, 1981, **47**, 1400.
5 P. Meakin, *Phys. Rev. Lett.*, 1983, **51**, 1119.
6 M. Kolb, R. Botet and R. Jullien, *Phys. Rev. Lett.*, 1983, **51**, 1123.
7 G. C. Ansell and E. Dickinson, *Phys. Rev. A*, 1987, **35**, 2349.
8 A. Hasmy, M. Foret, E. Anglaret, J. Pelous, R Vacher and R. Jullien, *J. Non-Cryst. Solids*, 1995, **186**, 118.
9 M. Lattuada, H. Wu, A. Hasmy and M. Morbidelli, *Langmuir*, 2003, **19**, 6312.
10 M. Rottereau, J. C. Gimel, T. Nicolai and D. Durand, *J. Eur. Phys. E*, 2004, **15**, 133.
11 R. C. Ball and R. Jullien, *J. Phys. Lett.*, 1984, **45**, L1031.
12 P. Meakin and M. Muthukumar, *J. Chem. Phys.*, 1989, **91**, 3212.
13 E. González Agustín and G. Ramírez-Santiago, *Phys. Rev. Lett.*, 1995, **74**, 1238.
14 E. Pefferkon and S. Stoll, *J. Colloid Interface Sci.*, 1990, **138**, 261.
15 C. Aubert and D. S. Cannell, *Phys. Rev. Lett.*, **56**, 738.
16 P. Dimon, S. K. Sinha, D. A. Weitz, C. R. Safinya, G. S. Smith, W. A. Varady and H. M. Lindsay, *Phys. Rev. Lett.*, 1986, **57**, 595.

17 P. Meakin and R. Jullien, *J. Phys. (Paris)*, 1985, **46**, 1543.
18 P. Meakin and R. Jullien, *J. Chem. Phys.*, 1988, **89**, 246.
19 A. Hasmy, M. Foret, J. Pelous and R. Jullien, *Phys. Rev. B: Condens. Matter*, 1993, **48**, 9345.
20 P. Meakin, *J. Chem. Phys.*, 1985, **83**, 3645.
21 M. Kolb, *J. Phys. A: Math. Gen.*, 1986, **19**, L263.
22 E. Dickinson, C. Elvingson and S. R. Euston, *J. Chem. Soc., Farady Trans.*, 1989, **85**, 891.
23 W. Y. Shih, I. A. Aksay and R. Kikuchi, *Phys. Rev. E.*, 1987, **36**, 5015.
24 M. D. Haw, M. Sievwright, W. C. K. Poon and P. N. Pusey, *Adv. Colloid Interface Sci.*, 1995, **62**, 1.
25 J. M. Jin, K. Parbhakar and L. H. Dao, *Phys. Rev. E*, 1996, **54**, 997.
26 T. Terao and T. Nakayama, *Phys. Rev. E*, 1998, **58**, 3490.
27 A. Fernández-Nieves, A. Fernández-Barbero, B. Vincent and F. J. de las Nieves, *Langmuir*, 2001, **17**, 1841.
28 M. Tirado-Miranda, A. Schmitt, J. Callejas-Fernández and A. Fernández-Barbero, *Langmuir*, 1999, **15**, 3437.
29 J. Liu, W. Y. Shih, M. Sarikaya and I. A. Aksay, *Phys. Rev. A*, 1990, **41**, 3206.
30 D. Frenkel and B. Smit, in *Understanding Molecular Simulation*, Computational Science Series, Academic Press, San Diego, 2nd edn., 1996, vol. 1.
31 M. D. Haw, M. Sievwright, W. C. K. Poon and P. N. Pusey, *Physica A*, 1995, **217**, 231 and references there in.
32 P. Meakin, in *Fractals, Scaling and Growth Far From Equilibrium*, Cambridge University Press, Cambridge, 1997.
33 P. Shurtenberger, personal communication.
34 E. González Agustín and Guillermo Ramírez-Santiago, *J. Colloid Interface Sci.*, 1996, **182**, 254.
35 M. Rottereau, J. C. Gimel, T. Nicolai and D. Durand, *Eur. Phys. J. E.*, 2004, **15**, 141.
36 S. Díez-Orrite, S. Stoll and P. Schurtenberger, in preparation.